A Finite-Element Method for Maxwell System Preserving Gauss Laws and Energy

Stéphanie Lala, Armel de Labourdonnaye

INRIA

INSTITUT NATIONAL DE RECHERCHE EN INFORMATIQUE ET EN AUTOMATIQUE

A finite-element method for Maxwell system preserving Gauss laws and Energy

Stéphanie Lala, Armel de La Bourdonnaye

N° 3557

Novembre 1998

THÈME 4

ISSN 0249-6399

INRIA
SOPHIA ANTIPOLIS

A finite-element method for Maxwell system preserving Gauss laws and Energy

Stéphanie Lala*, Armel de La Bourdonnaye*

Thème 4 — Simulation et optimisation
de systèmes complexes
Projet Caiman

Rapport de recherche n° 3557 — Novembre 1998 — 35 pages

Abstract: We present a finite-element method for simulating the time domain Maxwell system in 3 dimensions for unstructured meshes. The geometrical approach of the equations of electromagnetism leads to consider the fields as exterior differential forms tied together by the operator of differentiation by Hodge operator. The spatial discretization uses mixed finite-elements, and the temporal one uses a leap-frog scheme. For this method we show the following properties :
- it exactly preserves the Gauss laws and a discrete energy,
- on a regular mesh, it amounts to a finite difference scheme which is of order 2 in space an time,
- it preserves the Hamiltonian feature of Maxwell system which leads to interesting properties in long time computations.
The method is numerically tested on cavity modes for cubes and homogeneous or heterogeneous spheres. The results are compared to exact solutions. The method is also compared to a finite volume based software.

Key-words: differential geometry, mixed finite elements, electromagnetism, Maxwell system, numerical simulation, divergence preserving

* projet CAIMAN; E-mail : armel.de_La_bourdonnaye@sophia.inria.fr

Unité de recherche INRIA Sophia Antipolis
2004, route des Lucioles, B.P. 93, 06902 Sophia Antipolis Cedex (France)
Téléphone : 04 92 38 77 77 - International : +33 4 92 38 77 77 — Fax : 04 92 38 77 65 - International : +33 4 92 38 77 65

Une méthode d'éléments finis pour le système de Maxwell conservant les lois de Gauss et l'énergie

Résumé : Nous construisons une méthode en éléments finis pour la résolution du système de Maxwell en trois dimensions d'espace, dans le domaine temporel et pour des maillages non structurés. L'approche géométrique des équations de l'électromagnétisme, que nous adoptons, nous conduit à considérer les grandeurs physiques comme des p-formes différentielles liées par l'opérateur de différentiation extérieure et l'opérateur de Hodge. Nous discrétisons la partie spatiale par les éléments de Whitney, reformulés par Nédélec, et la partie temporelle par un schéma saute-mouton. Pour cette méthode, nous montrons les propriétés importantes suivantes :
- elle préserve exactement les lois de Gauss électrique et magnétique, ainsi qu'une énergie discrète.
- sur un maillage régulier, la méthode peut être vue comme un schéma aux différences finies. Nous montrons à l'aide des équations équivalentes qu'elle est alors d'ordre deux en temps et en espace.
- elle conserve le caractère hamiltonien du système de Maxwell. Les champs obtenus dérivent donc d'un quadripotentiel et minimisent un lagrangien discret, ce qui leur confère de bonnes propriétés pour des calculs en temps longs.

Nous validons la méthode obtenue sur la simulation de différents modes dans des cubes, des sphères homogènes ou hétérogènes. Nous comparons ces résultats aux solutions exactes. De plus, nous présentons les avantages et les inconvénients de cette méthode par rapport à une méthode de volumes finis commercialisée.

Mots-clés : géometrie différentielle, éléments finis mixtes, électromagnétisme, système de Maxwell, simulation numérique, conservation de la divergence

1 Introduction

Most of the time, numerical schemes discretizing Partial Differential Equations are studied from a local viewpoint, focusing on properties like consistency, stability, order of approximation in the limit of small time steps and spatial steps and so on. In the framework of Maxwell equations, we will derive a numerical method which aims at satisfying two global features of the continuous equations. The first one is the conservation of the electric charge and the nullity of the divergence of the magnetic field and comes from the fact that the exterior differentiation d satisfies $d \circ d = 0$. The second one is the fact the equations derive from the extremalization of a Lagrangian, leading to the conservation of a Hamiltonian which actually is the electromagnetic energy. In the first section, we show that these two features lie on differential geometry. Then, we propose a discretization lying on a discrete version of differential geometry. It is based on Whitney finite elements which have been adapted to numerical analysis by Raviart and Thomas [16], Nedelec [14] and Bossavit [4], for instance. The third section is devoted to the numerical analysis of the proposed discretization. In the last section we present numerical results of simulation.

We first remind Maxwell system, fix some notations and make some general remarks. We study

$$\begin{array}{ll} \frac{\partial B}{\partial t} + curl\, E = 0 & \text{Faraday} \\ \frac{\partial D}{\partial t} - curl\, H = J & \text{Ampère} \\ div\, D = \rho & \\ div\, B = 0 & \text{Gauss} \end{array} \tag{1}$$

where B is the magnetic induction, E the electric field, D the electric induction, H the magnetic field, J the density of electric current and ρ the density of electric charge. Since the conservation of electric charge equation

$$\frac{\partial \rho}{\partial t} + div J = 0 \tag{2}$$

is also fulfilled, one can see that Gauss laws are automatically satisfied, if they are satisfied at initial time. For this reason, they are generally not taken into account in numerical schemes, a consequence being that these laws are not numerically fulfilled (except on regular orthogonal meshes). This leads to

some non physical effects like creation of electric charge or artificial heating of plasmas when Maxwell system is coupled to transport equations for charged particles. Indeed, most of the schemes are using finite differences (FDTD) (see [24, 19] for instance). Finite Volume methods (FVTD) have also been developed, first based on a characteristics method (see Shankar, [17]) with conforming meshes and then modified to be simpler (see [15]).

Recently, FVTD methods inspired by Computational Fluid Dynamics have been developed for electromagnetism (see [6, 7]). Nevertheless, none of these methods exactly fulfills Gauss laws and energy conservation on general meshes. We just mention a penalisation method for FVTD (see [8]) which aims at diminishing the error on the divergence. We propose in the following a method based on differential geometry.

2 Differential geometry and Maxwell system

In this section, we remind some classical links between Maxwell system and exterior differential geometry.

In differential geometry, on space $\mathbb{R}^3$, one has differential forms of order p (p=0,1,2,3), which are p-skew symmetric linear forms over $\mathbb{R}^3$. We are going to link these forms with classical objects like functions and vector fields.

- A 0-form f is indeed a function : $\mathbb{R}^3 \mapsto \mathbb{R}$,
- A 1-form a is coupled with a vector field V_a^1 so that for $x \in \mathbb{R}^3$, $a(x)$: $U \mapsto V_a^1(x).U$,
- A 2-form b is coupled with a vector field V_b^2 so that for $x \in \mathbb{R}^3$, $b(x)$: $(U, V) \mapsto V_b^2(x).(U \wedge V)$,
- A 3-form F is linked with a function f_F so that for $x \in \mathbb{R}^3$, $F(x)$: $(U, V, W) \mapsto f_F(x)(U.(V \wedge W))$

where U, V, W denote here vector fields. With these forms, we present two operators which are of interest. The first one is the operator of exterior differentiation d, and the second one is the Hodge operator, denoted by $*$ in the sequel.

The exterior differentiation operates as follows.

- On 0-forms, it coincides with *gradient*,
- On 1-forms, it coincides with *curl*,
- On 2-forms, it coincides with *div*,
- On 3-forms, it is null.

We can check here the classical property $d \circ d = 0$. This property is of great importance in our case since it ensures that the divergence laws are fulfilled for all time.

The Hodge operator is involutive and couples p-forms and (3-p)-forms so that :

- for a 3-form F, $*F = f_F$,
- for a 1-form a, $V^2_{*a} = V^1_a$

which means, that a form and its Hodge transformed are associated to the same function or field.

Now, we have the Maxwell system presented in the introduction coupled with the medium constitutive laws :

$$\begin{array}{ll} \dfrac{\partial B}{\partial t} + curl E = 0 & \text{Faraday} \\ \dfrac{\partial D}{\partial t} - curl H = J & \text{Ampère} \\ div D = \rho & \text{Gauss} \\ div B = 0 & \\ D = \epsilon E & \text{Medium constitutive laws} \\ B = \mu H & \end{array} \tag{3}$$

A natural way to express this system with differential geometry is the following. Since they support a "curl" action, E and H are considered as 1-forms. In the same way, J, D and B are considered as 2-forms and ρ as a 3-form. So, the

system rewrites

$$\begin{array}{ll} \dfrac{\partial B}{\partial t} + dE = 0 & \text{Faraday} \\ \dfrac{\partial D}{\partial t} - dH = J & \text{Ampère} \\ dD = \rho & \text{Gauss} \\ dB = 0 & \\ D = *(\epsilon E) & \text{Medium constitutive laws} \\ B = *(\mu H) & \end{array} \tag{4}$$

This formalism will prove its efficiency in the sequel, since we will present a discretization which is an adapted version of the concepts of differential geometry we have presented in this section. Namely the relation $d \circ d$ will be also satisfied at the discrete level.

3 Discretization

In order to discretize the fields, we use mixed finite elements (see [14, 16] for instance). We consider a mesh $\mathcal{T}$ made of tetrahedra. We denote by α_i the edges of the mesh and by ϕ_i its faces. The 1-forms (E, H) are discretized with edge elements, and the 2-forms (B, D) are discretized with face elements. Hence, the *div* and *curl* operators are exactly implemented using Stokes formula, and so, the relation

$$div \circ curl = 0$$

is exactly fulfilled.

We now have to explain the most difficult part which is the discretization of the Hodge operator. But first, let us remark that we use as primary variables the fields D and B which are the conservative variables in the vocabulary of hyperbolic systems of conservation laws. Then, we compute E and H with Hodge operator, then we apply d to these fields and finally we increment the value of D and B. So we have to compute $*$ on 2-forms. Let b be a discrete 2-form. If a_i is a basis of edge functions (a_i is associated to edge α_i) and f_i is a basis of face functions (f_i is associated to face ϕ_i), b writes

$$b \sum_i b_i f_i \text{ with } \mathrm{b_i} \text{ real coefficients,}$$

$*b$ writes

$$*b \sum_j (*b)_j a_j \text{ with } (*\text{b})_\text{j} \text{ real coefficients}$$

and we look for the coefficients $(*b)_i$. We discretize Hodge operator weakly. Then

$$\langle *b,\ a_i \rangle = \langle b, a_i \rangle \text{ for all a}_\text{i} \text{ in the basis of edges functions}$$

Where $\langle ..., ... \rangle$ stands for the L^2 scalar product. We then have

$$(\langle a_i,\ a_j \rangle)((*b)_j) = (\langle a_i,\ f_k \rangle)(b_k).$$

Hence, denoting by $M_{1,1}$ the Mass matrix of edge functions :

$$M_{1,1_{i,j}} = \langle a_i,\ a_j \rangle$$

and by $M_{1,2}$ the matrix coupling edge and face functions :

$$M_{1,2_{i,j}} = \langle a_i,\ f_j, \rangle$$

we can see that the matrix M_* which corresponds to the discrete Hodge operator is

$$M_* = M_{1,1}^{-1} M_{1,2}.$$

The last point of this section is to present the time discretization. We use a classical leap-frog scheme.

$$\begin{cases} B^{n+\frac{1}{2}} = B^{n-\frac{1}{2}} - \Delta t d \frac{*}{\varepsilon} D^n \\ D^{n+1} = D^n + \Delta t d \frac{*}{\mu} B^{n+\frac{1}{2}} - \Delta t J^{n+\frac{1}{2}} \end{cases} \tag{5}$$

We have to point out here that our scheme is implicit since the discrete Hodge operator requires to solve a linear system. Nonetheless all the usual ways we know to precisely control the divergence laws are implicit (see [2, 12]). But here we have only to solve a Mass-Matrix instead of a Poisson problem as in the case of the above referenced methods.

4 Numerical analysis

In this section, we will study the numerical properties of the scheme presented above. First, viewing it as a finite difference scheme, we will compute its "modified equation" (see [21, 1, 18]) in order to evaluate the accuracy of the scheme in time and space. Then, we will show that our scheme preserves a numerical energy and the divergences of the conservative fields D and B. Finally, we will show that the numerical solutions of our system derive from a discrete quadripotential which minimizes a numerical Lagrangian.

4.1 Modified equation

In order to study the stability and the accuracy of the scheme presented in this paper, we will view it as a finite-difference one. Thus, we change a little our spatial discretization and use a regular parallelepipedic mesh with the associated mixed finite elements (see [14]). Let us remind that the modified equation is the partial differential equation which is exactly satisfied by the discrete fields. An exhaustive but fastidious computation of this equation is presented in [13] and uses a technique developed in [5] and symbolic calculus tools. The result is that the modified equation is :

$$\begin{aligned} \frac{\partial B}{\partial t} + dE &= \mathcal{O}(\Delta x^2,\ \Delta t^2) \\ \frac{\partial D}{\partial t} - dH &= \mathcal{O}(\Delta x^2,\ \Delta t^2) \end{aligned} \tag{6}$$

It follows that our scheme is an order 2 scheme, both in time and space. Let us stress on the fact that the proof of this result does not require the mesh to be orthogonal but only to be regular (i.e. the cells are all the same parallelepiped).

4.2 Divergence laws

We show the proposition

Proposition 1 *if* $B^{1/2} = 0$, *then* $dB^{n-1/2} = divB^{n-1/2} = 0$ *for all* $n > 0$.
if $D^0 = \rho^0$ *and* $divJ^{n+1/2} + \dfrac{\rho^{n+1} - \rho^n}{\Delta t} = 0$, *then* $D^n = \rho^n$ *for all* $n > 0$.

Proof :
Indeed, we remind that our discrete *curl* and *div* are the exact continuous operators and satisfy $div \circ curl = 0$. Hence, since $B^{n+1/2} = B^{n-1/2} - \Delta t curl(\frac{*}{\epsilon} D^n)$, we obtain

$$divB^{n+1/2} = divB^{n-1/2}.$$

By induction , if $B^{1/2} = 0$, $B^{n+1/2} = 0$, $for\ all\ n$.

Similarly, since $D^{n+1} = D^n + \Delta t curl(\frac{*}{\mu} B^{n+1/2}) - \Delta t J^{n+1/2}$, we obtain that $divD^{n+1} = divD^n - \Delta t div J^{n+1/2}$.
Using discrete charge conservation law one has $divD^{n+1} = divD^n + \rho^{n+1} - \rho^n$. So

$$divD^{n+1} - \rho^{n+1} = divD^n - \rho^n.$$

By induction, if $divD^0 - \rho^0 = 0$, then $divD^n - \rho^n = 0$, $for\ all\ n$. □

4.3 Conservation of energy

In this section, we show that there is a approximate energy which is exactly preserved by the scheme. We stress on the fact that this is better than approximately preserving the exact energy. Let

$$\mathcal{E}^n = \int_{\mathcal{M}} D^n.E^n + B^{n-1/2}.H^{n-1/2} - \Delta t dH^{n-1/2}.E^n$$

Here $\mathcal{M}$ denotes the domain of computation and we suppose that we have metallic boundary conditions. We remark that it can be rewritten as :

$$\mathcal{E}^n = \int_{\mathcal{M}} D^n.E^n + \frac{B^{n-1/2}.H^{n+1/2} + B^{n+1/2}.H^{n-1/2}}{2}$$

With this notation, it is clear that $\mathcal{E}^n$ is symmetric with respect to the fields, and is an order 2 approximation of the continuous energy. We show the

Proposition 2 *The energy $\mathcal{E}^n$ is preserved by our scheme.*

Proof :
The first point is to prove that if a and b are discrete 1-forms, then the duality product $< \star a, b >$ is a symmetric bilinear form. Indeed, let $a = \sum \alpha_i a_i$ and $b = \sum \beta_i a_i$. The product $< \star a, b >$ is expressed by

$$< \star a, b >= (\beta_i)^T M_{1,2}^T M_{1,1}^{-1} M_{1,2}(\alpha_j)$$

Matrices $M_{1,1}$ and $M_{1,2}$ are the ones presented in the discretization of Hodge operator. On this expression, the symmetry is obvious.

Now we can prove that $\mathcal{E}^{n+1} - \mathcal{E}^n = 0$. First we rewrite the energy using fields D and B only.

$$\mathcal{E}^n = \int_{\mathcal{M}} D^n . \frac{\star D^n}{\varepsilon} + B^{n-\frac{1}{2}} . \frac{\star B^{n-\frac{1}{2}}}{\mu} - \Delta t \frac{d \star B^{n-\frac{1}{2}}}{\mu} . \frac{\star D^n}{\varepsilon} \tag{7}$$

and energy at time $(n+1)\,\Delta t$, denoted by $\mathcal{E}^{n+1}$,writes :

$$\mathcal{E}^{n+1} = \int_{\mathcal{M}} D^{n+1} . \frac{\star D^{n+1}}{\varepsilon} + B^{n+\frac{1}{2}} . \frac{\star B^{n+\frac{1}{2}}}{\mu} - \Delta t \frac{d \star B^{n+\frac{1}{2}}}{\mu} . \frac{\star D^{n+1}}{\varepsilon} \tag{8}$$

Since

$$D^{n+1} = D^n + \Delta t \frac{d\star}{\mu} B^{n+\frac{1}{2}} + \Delta t J^{n+\frac{1}{2}},$$

one has :

$$\begin{aligned} \mathcal{E}^{n+1} = \int_{\mathcal{M}} & \left(D^n + \Delta t \frac{d \star B^{n+\frac{1}{2}}}{\mu} \right) . \left(\frac{\star D^n}{\varepsilon} + \Delta t \frac{\star d \star B^{n+\frac{1}{2}}}{\varepsilon \mu} \right) \\ & + B^{n+\frac{1}{2}} . \frac{\star B^{n+\frac{1}{2}}}{\mu} \\ & - \Delta t \frac{d \star B^{n+\frac{1}{2}}}{\mu} . \left(\frac{\star D^n}{\varepsilon} + \Delta t \frac{\star d \star B^{n+\frac{1}{2}}}{\varepsilon \mu} \right) \end{aligned} \tag{9}$$

As order 2 terms cancel, one obtains

$$\begin{aligned}\mathcal{E}^{n+1} = \int_{\mathcal{M}} \quad & D^n.\frac{\star D^n}{\varepsilon} + \Delta t \left(\frac{D^n.\star d \star B^{n+\frac{1}{2}}}{\varepsilon\mu} + \frac{\star D^n.d \star B^{n+\frac{1}{2}}}{\varepsilon\mu} \right) \\ & + B^{n+\frac{1}{2}}.\frac{\star B^{n+\frac{1}{2}}}{\mu} - \Delta t \frac{d \star B^{n+\frac{1}{2}}.\star D^n}{\mu\varepsilon}\end{aligned} \tag{10}$$

Using the symmetry property of the discrete Hodge operator,

$$\mathcal{E}^{n+1} = \int_{\mathcal{M}} D^n.\frac{\star D^n}{\varepsilon} + \Delta t \frac{D^n.\star d \star B^{n+\frac{1}{2}}}{\varepsilon\mu} + B^{n+\frac{1}{2}}.\frac{\star B^{n+\frac{1}{2}}}{\mu} \tag{11}$$

Using the discrete Faraday law :

$$B^{n+\frac{1}{2}} = B^{n-\frac{1}{2}} - \Delta t \frac{d\star}{\varepsilon} D^n, \tag{12}$$

One has :

$$\begin{aligned}\mathcal{E}^{n+1} = \int_{\mathcal{M}} \quad & D^n.\frac{\star D^n}{\varepsilon} + \Delta t \frac{D^n.\left(\star d \star B^{n-\frac{1}{2}} - \Delta t \star d \star \frac{d\star}{\varepsilon} D^n \right)}{\varepsilon\mu} \\ & + \left(B^{n-\frac{1}{2}} - \Delta t \frac{d \star D^n}{\varepsilon} \right) . \left(\frac{\star B^{n-\frac{1}{2}}}{\mu} - \Delta t \frac{\star d \star D^n}{\varepsilon\mu} \right)\end{aligned} \tag{13}$$

Here also, the order 2 terms cancel. So,

$$\begin{aligned}\mathcal{E}^{n+1} = \int_{\mathcal{M}} \quad & D^n.\frac{\star D^n}{\varepsilon} + \Delta t \frac{D^n.\star d \star B^{n-\frac{1}{2}}}{\varepsilon\mu} + B^{n-\frac{1}{2}}.\frac{\star B^{n-\frac{1}{2}}}{\mu} \\ & - \Delta t \left(\frac{B^{n-\frac{1}{2}}.\star d \star D^n}{\varepsilon\mu} + \frac{d \star D^n.\star B^{n-\frac{1}{2}}}{\varepsilon\mu} \right)\end{aligned} \tag{14}$$

Integrating by part, one has :

$$\mathcal{E}^{n+1} = \int_{\mathcal{M}} D^n.\frac{\star D^n}{\varepsilon} + B^{n-\frac{1}{2}}.\frac{\star B^{n-\frac{1}{2}}}{\mu} - \Delta t \frac{d \star B^{n-\frac{1}{2}}.\star D^n}{\varepsilon\mu} = \mathcal{E}^n \tag{15}$$

So discrete energy at time $(n+1)\,\Delta t$ is equal to discrete energy at time $n\Delta t$:

$$\boxed{\mathcal{E}^{n+1} = \mathcal{E}^n \quad \forall n} \tag{16}$$

□

Let us remark here that the discrete energy is a good approximation of the continuous one when the time step is small. Nevertheless, it is generally not a positive form. So we have a Courant-Freidrichs-Levy condition to ensure that $\mathcal{E}^n$ is positive so that the preservation of this energy implies the stability of the scheme.

4.4 Quadripotential and Lagrangian

In order to obtain a long time quality for our scheme, we want to show that it has the same global features as the continuous Maxwell system. Here, we will show that the fields $B^{n+1/2}$ and E^n derive from a quadripotential $(A^{n+1/2},\ V^n)$ in the following sense :

$$B^{n-\frac{1}{2}} = dA^{n-\frac{1}{2}}$$

and

$$E^n = \frac{A^{n+\frac{1}{2}} - A^{n-\frac{1}{2}}}{\Delta t} - dV^n,$$

using only

$$\frac{B^{n+\frac{1}{2}} - B^{n-\frac{1}{2}}}{\Delta t} + dE^n = 0$$

and

$$dB^{n+\frac{1}{2}} = 0$$

Here, $A^{n+1/2}$ is a 1-form (discretized on an edge element basis) and V^n is a 0-form (discretized on a P1-Lagrange basis). We will then show that $(A^{n+1/2},\ V^n)_n$ is an extremum of a discrete Lagrangian which approximates the continuous one.

We begin by reminding the following result.

Proposition 3 *If f is a discrete closed p-form (that is to say $df = 0$), then it is an exact discrete form in the sense that there exists a discrete (p-1)-form g such that $dg = p$.*

On the continuous level, it is an old and classical result of cohomology. Here, the original part is to prove that g belongs to the set of discrete forms. The proof is done by exhibiting an isomorphism between discrete forms and simplexes of the mesh and using a classical result of simplicial homology (see [10, 20]). For a detailed proof, one can refer to [13]. We are now able to prove the

Proposition 4 *The fields E and B solutions of the discrete scheme discretely derive from a quadripotential, that is to say, if $B^{n+1/2}$ and E^n satisfy*

$$\frac{B^{n+\frac{1}{2}} - B^{n-\frac{1}{2}}}{\Delta t} + d\ E^n = 0 \tag{17}$$

and

$$dB^{n+\frac{1}{2}} = 0 \tag{18}$$

Then, there exists a discrete 1-form $A^{n-\frac{1}{2}}$ and a discrete 0-form V^n such that

$$B^{n+\frac{1}{2}} = dA^{n+\frac{1}{2}}$$

and

$$E^n = -\frac{A^{n+\frac{1}{2}} - A^{n-\frac{1}{2}}}{\Delta t} + dV^n$$

Proof :
The proof of the proposition relies on the discrete exactness of the closed discrete forms. Indeed, using (17) one can deduce that there exists a discrete 1-form $A^{n+\frac{1}{2}}$ such that :

$$B^{n+\frac{1}{2}} = dA^{n+\frac{1}{2}} \quad \forall n$$

This implies that :

$$\frac{B^{n+\frac{1}{2}} - B^{n-\frac{1}{2}}}{\Delta t} + dE^n = 0$$

which rewrites :

$$\frac{dA^{n+\frac{1}{2}} - dA^{n-\frac{1}{2}}}{\Delta t} + dE^n = 0$$

or

$$d\left(\frac{A^{n+\frac{1}{2}} - A^{n-\frac{1}{2}}}{\Delta t} + E^n\right) = 0.$$

Again using discrete exactness of closed discrete forms, we finally derive that there is a discrete 0-form V^n such that

$$\frac{A^{n+\frac{1}{2}} - A^{n-\frac{1}{2}}}{\Delta t} + E^n = dV^n \quad \forall n$$

that is to say :

$$E^n = -\frac{A^{n+\frac{1}{2}} - A^{n-\frac{1}{2}}}{\Delta t} + dV^n$$

which completes the proof. □

We are now going to show that the discrete quadripotential is an extremum of a discrete Lagrangian. The continuous Lagrangian corresponding to Maxwell system is

$$\mathcal{L}_c = \int_t \int_{\mathcal{M}} E(t).D(t) - H(t).B(t)$$

or

$$\mathcal{L}_c = \int_t \int_{\mathcal{M}} E(t).\varepsilon \star E(t) - \frac{\star}{\mu} B(t).B(t)$$

We propose as a discrete Lagrangian :

$$\mathcal{L} = \sum_n \int_{\mathcal{M}} E^n.\varepsilon \star E^n - \frac{\star}{\mu} B^{n-\frac{1}{2}}.B^{n-\frac{1}{2}}$$

Using the quadripotential derived from the previous proposition, it rewrites :

$$\begin{aligned}\mathcal{L} = & \sum_n \int_{\mathcal{M}} \left(-\frac{A^{n+\frac{1}{2}} - A^{n-\frac{1}{2}}}{\Delta t} + dV^n \right) .\varepsilon \star \left(-\frac{A^{n+\frac{1}{2}} - A^{n-\frac{1}{2}}}{\Delta t} + dV^n \right) \\ - & \sum_n \int_{\mathcal{M}} \frac{\star}{\mu} \left(dA^{n-\frac{1}{2}} \right) . \left(dA^{n-\frac{1}{2}} \right)\end{aligned}$$

We will show the

Proposition 5 *The quadripotential $A^{n+1/2}, V^n$ is an extremum of the Lagrangian $\mathcal{L}$ if the fields D^n and $H^{n+1/2}$ satisfy :*

$$\frac{D^{n+1} - D^n}{\Delta t} - dH^{n+\frac{1}{2}} = 0$$

and

$$dD^n = 0$$

Proof :
We want to check that the quadripotential satisfies

$$\delta\mathcal{L} = \frac{\partial \mathcal{L}}{\partial A}\delta A + \frac{\partial \mathcal{L}}{\partial V}\delta V = 0$$

for all variations $(\delta A, \delta V)$ of the quadripotential. One has that :

$$\begin{aligned}\delta\mathcal{L} = & 2\sum_n \int_{\mathcal{M}} \left(-\frac{A^{n+\frac{1}{2}} - A^{n-\frac{1}{2}}}{\Delta t} + dV^n \right) .\varepsilon \star \left(-\frac{\delta A^{n+\frac{1}{2}} - \delta A^{n-\frac{1}{2}}}{\Delta t} + d\delta V^n \right) \\ - & 2\sum_n \int_{\mathcal{M}} \left(dA^{n-\frac{1}{2}} \right) . \frac{\star}{\mu} \left(d\delta A^{n-\frac{1}{2}} \right)\end{aligned}$$

Integrating by part, one obtains :

$$\begin{aligned}\delta\mathcal{L} = & \quad 2\sum_n \int_{\mathcal{M}} \delta A^{n+\frac{1}{2}}.\frac{\varepsilon\star}{\Delta t}\left(\frac{A^{n+\frac{1}{2}}-A^{n-\frac{1}{2}}}{\Delta t} - dV^n\right) \\ & + \quad 2\sum_n \int_{\mathcal{M}} \delta A^{n-\frac{1}{2}}.\left(\frac{\varepsilon\star}{\Delta t}\left(-\frac{A^{n+\frac{1}{2}}-A^{n-\frac{1}{2}}}{\Delta t} + dV^n\right) + d\frac{\star}{\mu}dA^{n-\frac{1}{2}}\right) \\ & + \quad 2\sum_n \int_{\mathcal{M}} \delta V^n.\varepsilon d\star\left(-\frac{A^{n+\frac{1}{2}}-A^{n-\frac{1}{2}}}{\Delta t} + dV^n\right)\end{aligned}$$

Since we have :

$$\begin{aligned}&\sum_n \int_{\mathcal{M}} \delta A^{n-\frac{1}{2}}.\left(\frac{\varepsilon\star}{\Delta t}\left(-\frac{A^{n+\frac{1}{2}}-A^{n-\frac{1}{2}}}{\Delta t} + dV^n\right) + d\frac{\star}{\mu}dA^{n-\frac{1}{2}}\right) \\ &\quad = \sum_n \int_{\mathcal{M}} \delta A^{n+\frac{1}{2}}.\left(\frac{\varepsilon\star}{\Delta t}\left(-\frac{A^{n+\frac{3}{2}}-A^{n+\frac{1}{2}}}{\Delta t} + dV^{n+1}\right) + d\frac{\star}{\mu}dA^{n+\frac{1}{2}}\right)\end{aligned},$$

the condition of extremalization writes :

$$\begin{aligned}\delta\mathcal{L} = & \quad 2\sum_n \int_{\mathcal{M}} \delta A^{n+\frac{1}{2}}.\frac{\varepsilon\star}{\Delta t}\left(\frac{-A^{n+\frac{3}{2}}+2A^{n+\frac{1}{2}}-A^{n-\frac{1}{2}}}{\Delta t} + d\left(V^{n+1}-V^n\right)\right) \\ & + \quad 2\sum_n \int_{\mathcal{M}} \delta A^{n+\frac{1}{2}}.\frac{\varepsilon\star}{\Delta t}d\frac{\star}{\mu}dA^{n+\frac{1}{2}} \\ & + \quad 2\sum_n \int_{\mathcal{M}} \delta V^n.\varepsilon d\star\left(-\frac{A^{n+\frac{1}{2}}-A^{n-\frac{1}{2}}}{\Delta t} + dV^n\right)\end{aligned}.$$

That is to say :

$$\begin{aligned}\delta\mathcal{L} = \quad & 2\sum_n \int_{\mathcal{M}} \delta A^{n+\frac{1}{2}}.\varepsilon \star \left(\frac{\frac{-A^{n+\frac{3}{2}} + A^{n+\frac{1}{2}}}{\Delta t} - \frac{-A^{n+\frac{1}{2}} + A^{n-\frac{1}{2}}}{\Delta t}}{\Delta t} \right) \\ + \quad & 2\sum_n \int_{\mathcal{M}} \delta A^{n+\frac{1}{2}}.\varepsilon \star \frac{dV^{n+1} - dV^n}{\Delta t} \\ + \quad & 2\sum_n \int_{\mathcal{M}} \delta A^{n+\frac{1}{2}}.\varepsilon \star d\frac{\star}{\mu} B^{n+\frac{1}{2}} \\ + \quad & 2\sum_n \int_{\mathcal{M}} \delta V^n.\varepsilon d \star \left(-\frac{A^{n+\frac{1}{2}} - A^{n-\frac{1}{2}}}{\Delta t} + dV^n \right)\end{aligned}$$

which rewrites :

$$\begin{aligned}\delta\mathcal{L} = \quad & 2\sum_n \int_{\mathcal{M}} \delta A^{n+\frac{1}{2}}. \left(\varepsilon \star \left(\frac{-E^{n+1} + E^n}{\Delta t} \right) + dH^{n+\frac{1}{2}} \right) \\ + \quad & 2\sum_n \int_{\mathcal{M}} \delta V^n.d\varepsilon \star E^n\end{aligned}$$

Hence :

$$\begin{aligned}\delta\mathcal{L} = \quad & 2\sum_n \int_{\mathcal{M}} \delta A^{n+\frac{1}{2}}. \left(- \left(\frac{D^{n+1} - D^n}{\Delta t} - dH^{n+\frac{1}{2}} \right) \right) \\ + \quad & 2\sum_n \int_{\mathcal{M}} \delta V^n.dD^n\end{aligned}$$

Assuming $H^{n+1/2}$ and D^n satisfy

$$\begin{cases} \dfrac{D^{n+1} - D^n}{\Delta t} - dH^{n+\frac{1}{2}} = 0 \\ dD^n = 0 \end{cases},$$

one finally obtains :

$$\boxed{\delta\mathcal{L} = 0 \quad \forall \delta A^{n+\frac{1}{2}} \text{ et } \forall \delta V^n}$$

This ends the proof. □

5 Numerical experiments

In this section, we presents numerical tests of our method in order to check the properties presented in the previous section. The chosen tests are computations of eigenmodes of cavities. They generally are tough tests because of the possible comparison with an analytic solution and because of the possibility of long time simulations.

5.1 Eigenmode of a metallic cubic cavity

5.1.1 The test case

we consider a cubic cavity of size $L = 1$. We simulate the mode (1,1,1) for which fields E and B are defined by

$$E = \cos(\omega t) \begin{pmatrix} A_1 \cos\left(\frac{k_1 \pi x}{L}\right) \sin\left(\frac{k_2 \pi y}{L}\right) \sin\left(\frac{k_3 \pi z}{L}\right) \\ A_2 \sin\left(\frac{k_1 \pi x}{L}\right) \cos\left(\frac{k_2 \pi y}{L}\right) \sin\left(\frac{k_3 \pi z}{L}\right) \\ A_3 \sin\left(\frac{k_1 \pi x}{L}\right) \sin\left(\frac{k_2 \pi y}{L}\right) \cos\left(\frac{k_3 \pi z}{L}\right) \end{pmatrix}$$

and

$$B = \frac{1}{c} \sin(\omega t) \begin{pmatrix} B_1 \sin\left(\frac{k_1 \pi x}{L}\right) \cos\left(\frac{k_2 \pi y}{L}\right) \cos\left(\frac{k_3 \pi z}{L}\right) \\ B_2 \cos\left(\frac{k_1 \pi x}{L}\right) \sin\left(\frac{k_2 \pi y}{L}\right) \cos\left(\frac{k_3 \pi z}{L}\right) \\ B_3 \cos\left(\frac{k_1 \pi x}{L}\right) \cos\left(\frac{k_2 \pi y}{L}\right) \sin\left(\frac{k_3 \pi z}{L}\right) \end{pmatrix}$$

with

$$k = \begin{pmatrix} k_1 \\ k_2 \\ k_3 \end{pmatrix} = \begin{pmatrix} 1 \\ 1 \\ 1 \end{pmatrix},$$

$$A = \begin{pmatrix} -1 \\ 0 \\ 1 \end{pmatrix} \text{ and } B = \begin{pmatrix} \frac{-1}{\sqrt{3}} \\ \frac{2}{\sqrt{3}} \\ \frac{-1}{\sqrt{3}} \end{pmatrix}$$

5.1.2 Spatial comparison

On figures (1) and (2) we present exact and approximated solutions after 10 periods. We can observe the good quality of the results. The mesh step is about the wavelength divided by 21. We remark here that the main differences

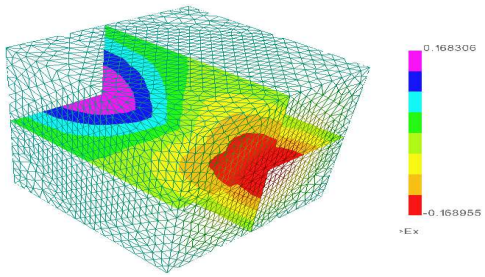

Computed solution

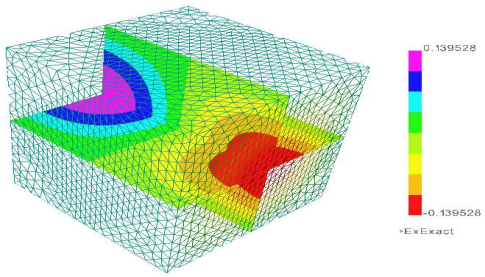

Exact solution

Figure 1: x component of the electric field after 10 periods.

between exact and computed solutions are due to the error of approximation of the initial solution corresponding to the analytic value of the mode (see [13] for more details).

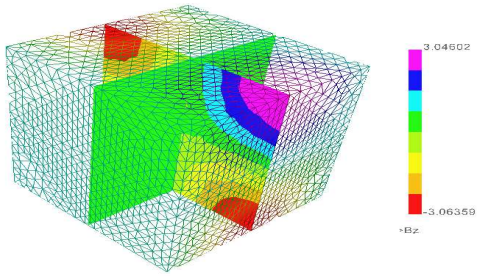

Computed solution

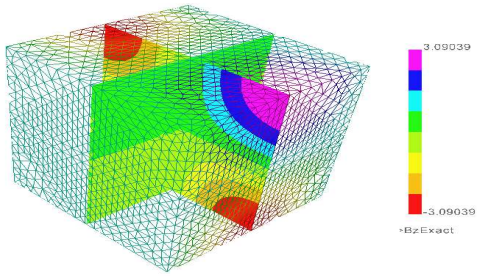

Exact solution

Figure 2: z component of the magnetic induction after 10 periods.

5.1.3 Time evolution

For a given point we present the time evolution of the solution called "Hodge solution" in the following. This will help us to obtain more precise comparisons. We use a mesh with 6724 points. This approximately amounts to 20 points by wavelength. It is a correct evolution though a little dispersive, in accordance with the order 2 approximation of our scheme. On figure 4, we present a long time simulation. We have checked that we loose half a period for 125 periods. This amounts to a dispersion of 0.4 %. We can also observe the good quality of our scheme for long times. This is generally not the case for methods able to handle arbitrary meshes. In the following plots we vary the number of points by wavelength for the same mesh as above (it means that we change the frequency). We observe that 10 points by wavelength is necessary

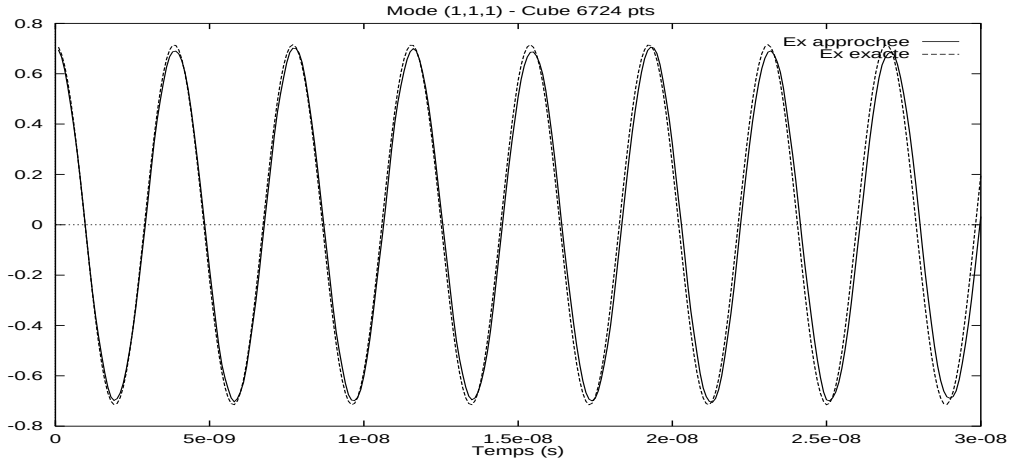

Figure 3: Evolution of the electric field (20 points by wavelength).

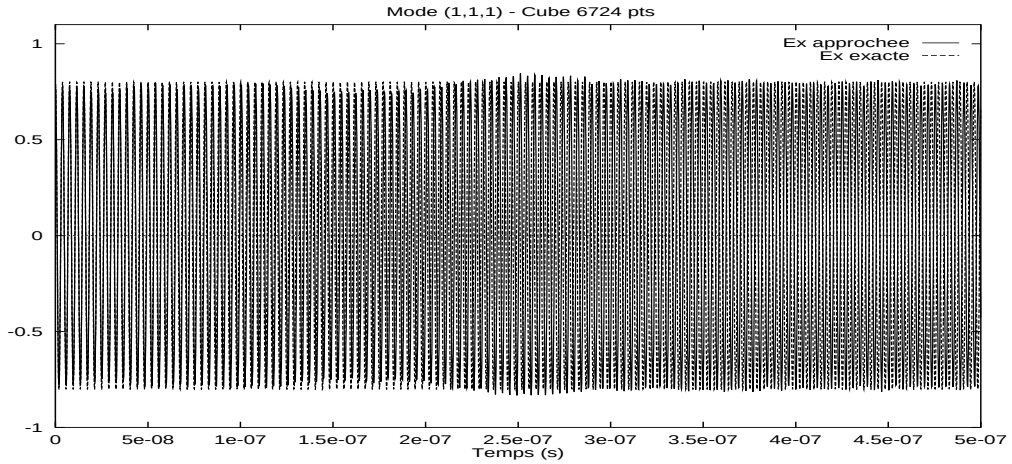

Figure 4: long time evolution of the electric field.

to obtain a reasonable solution. Now we compare our method with a finite volume one (see [3] for details) on the (1,1,-2) mode. We begin by comparing the two methods on the same mesh. The results observed on figure 9 seem to indicate that our method has the same order of magnitude for dispersion as the modified order 3 Finite Volume code and is less diffusive. Nonetheless, it is not a fair comparison since memory and computation costs are more important

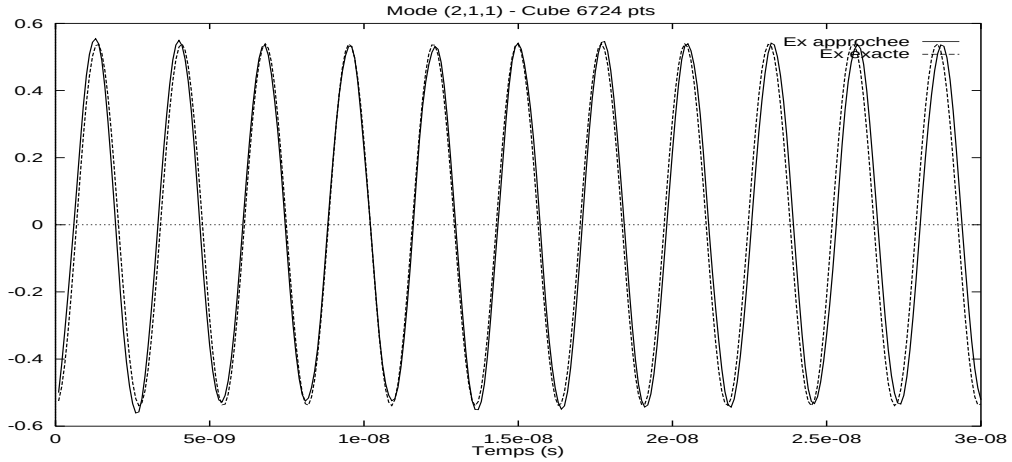

Figure 5: Evolution of the electric field (15 points by wavelength).

for the finite element method. It is why it is more honest to compare finite volume results to ours obtained on a mesh having 2.5 times less points. With this ratio, memory and computation costs are equivalent for the two methods. On figure 10 one can observe results which are really similar on short times.

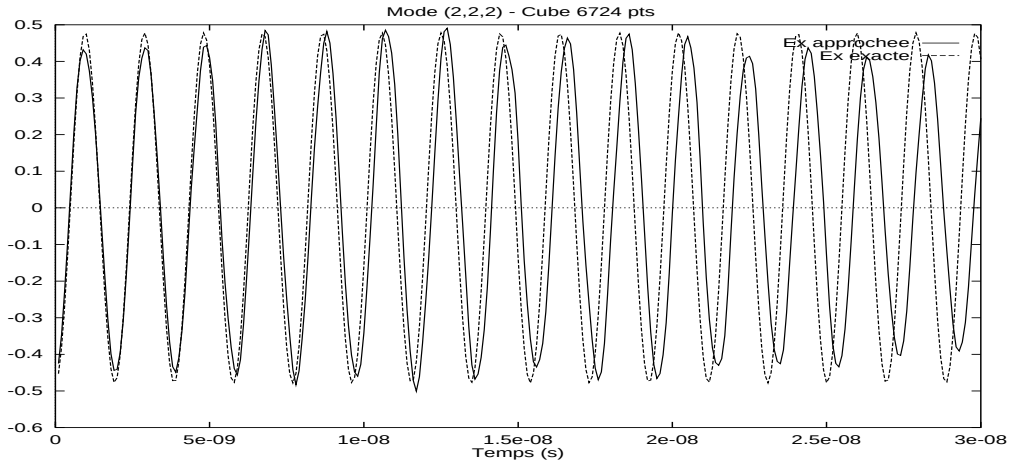

Figure 6: Evolution of the electric field (11 points by wavelength).

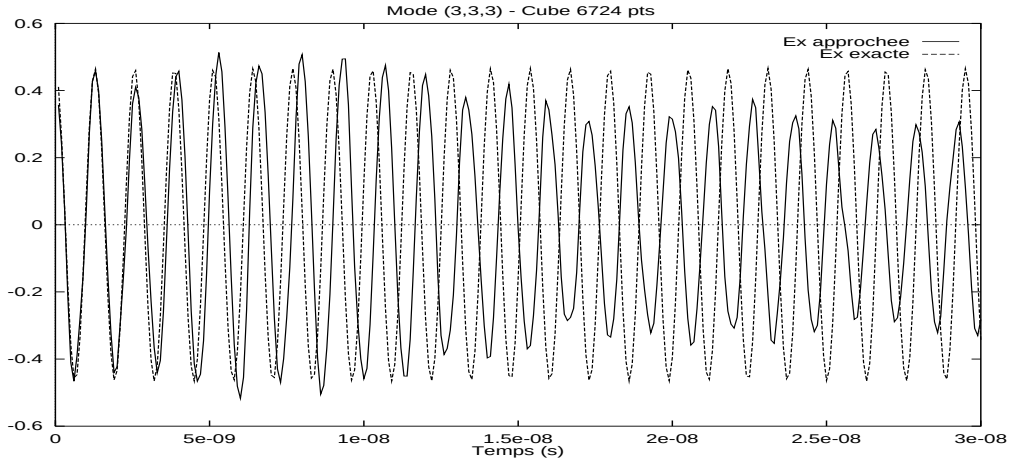

Figure 7: Evolution of the electric field (7 points by wavelength).

Nevertheless, our method is more dispersive. It confirms that is of order 2 in space. One can also observe that for long times our method is less diffusive.

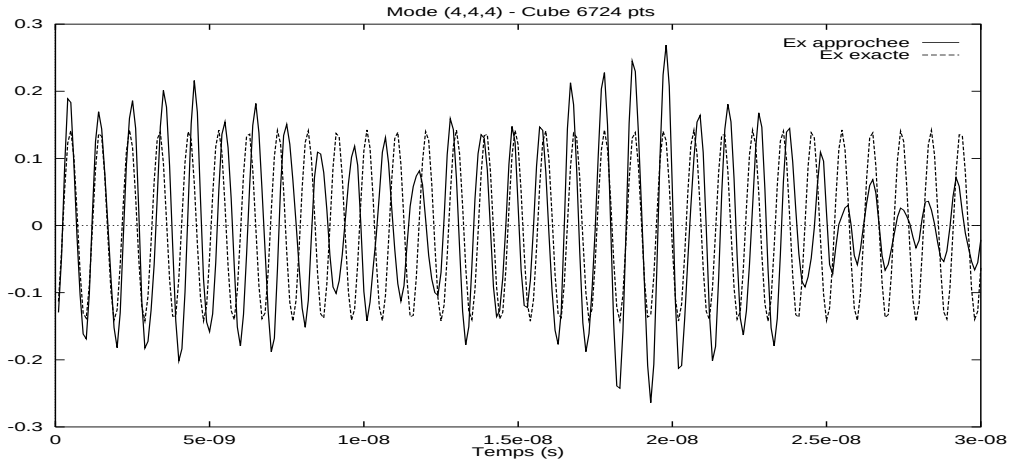

Figure 8: Evolution of the electric field (5 points by wavelength).

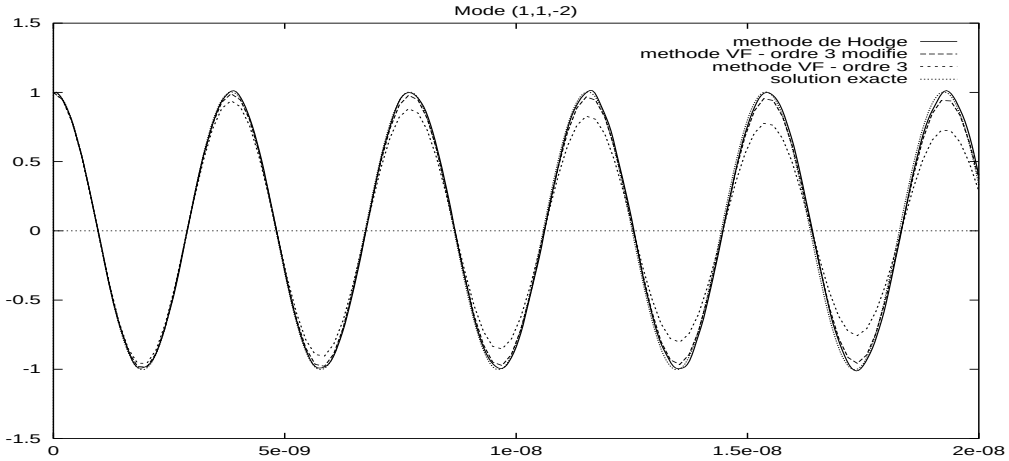

Figure 9: Comparison with a finite volume method on the same mesh.

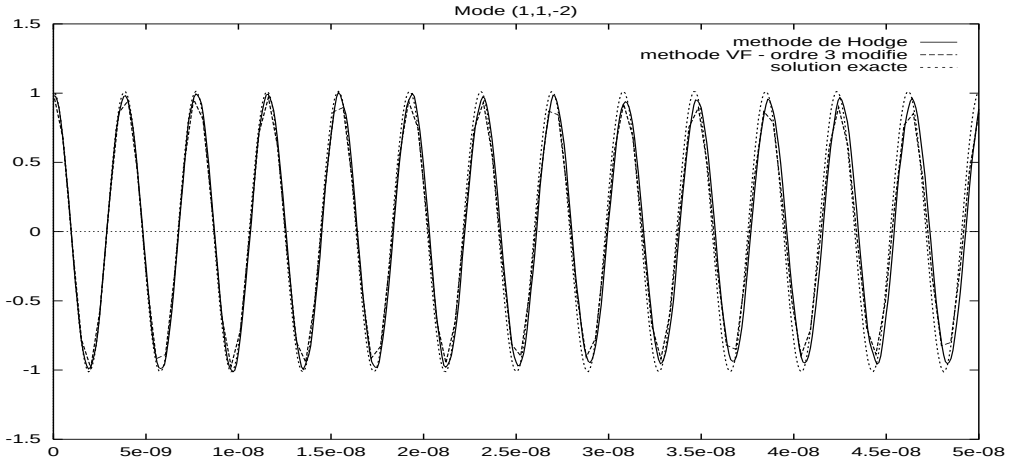

Figure 10: Comparison with a finite volume method for similary costs.

5.2 Eigenmode of a metallic homogeneous spherical cavity

5.2.1 The test case

We are going to study a resonance problem in a spherical cavity of radius 1. We choose the wave number k to be the first 0 of the spherical Bessel function j_1. The simulated mode is given by

$$\left\{\begin{array}{rcccl} E_x &=& \cos(\omega t) & \frac{y}{r^2} & \left(\frac{\sin(kr)}{kr} - \cos(kr)\right) \\ E_y &=& \cos(\omega t) & \frac{-x}{r^2} & \left(\frac{\sin(kr)}{kr} - \cos(kr)\right) \\ E_z &=& 0 & & \end{array}\right.$$

and

$$\left\{\begin{array}{rcccl} Hx &=& \frac{\sin(\omega t)}{\omega\mu} & \frac{xz}{r^4} & \left(\sin(kr)\left(\frac{3}{kr} - kr\right) - 3\cos(kr)\right) \\ Hy &=& \frac{\sin(\omega t)}{\omega\mu} & \frac{yz}{r^4} & \left(\sin(kr)\left(\frac{3}{kr} - kr\right) - 3\cos(kr)\right) \\ Hz &=& \frac{\sin(\omega t)}{\omega\mu} & \left\{\frac{z^2}{r^4}\right. & \left(\sin(kr)\left(\frac{3}{kr} - kr\right) - 3\cos(kr)\right) \\ & & & \frac{-1}{r^2} & \left.\left(\sin(kr)\left(\frac{1}{kr} - kr\right) - \cos(kr)\right)\right\} \end{array}\right.$$

where (x, y, z) are the cartesian coordinates of $\mathbb{R}^3$ and

$$r = \sqrt{x^2 + y^2 + z^2}$$

5.2.2 Spatial comparison

Now we compare the simulation on this mode with its analytical value. Once again the picture shows a good quality of the simulation.

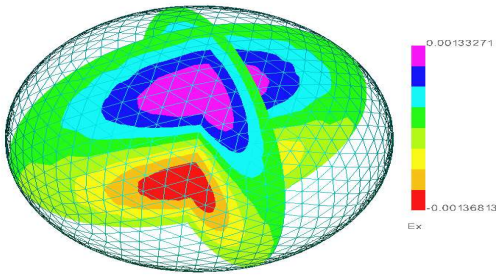

Computed solution

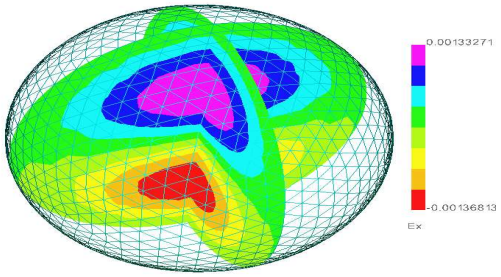

Exact solution

Figure 11: x component of the electric field after 5 periods.

5.2.3 Temporal comparison

On figure 12 one can observe that our scheme gives correct results. We remark that here, our mesh has 8905 points. This corresponds to about 6 points by wavelength (here the wavelength is 0.445).

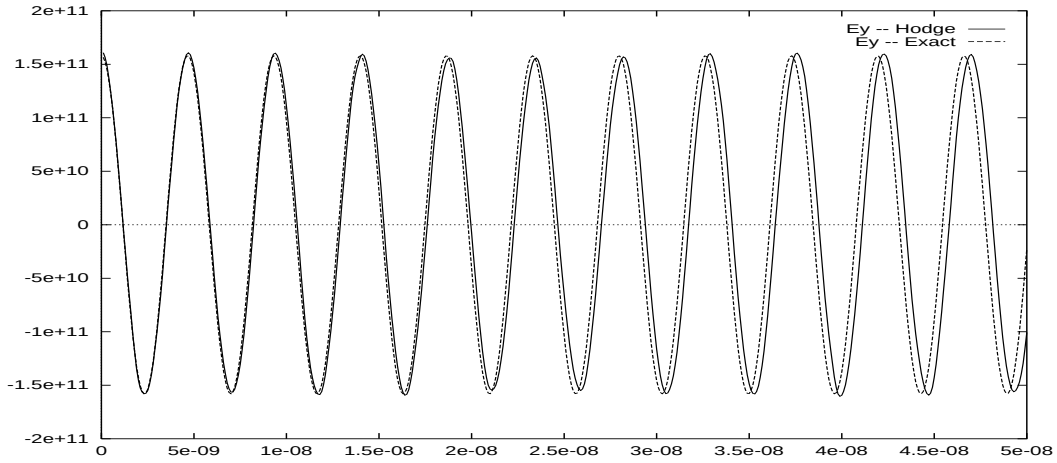

Figure 12: y component of the electric field.

5.3 Eigenmode of a metallic heterogeneous spherical cavity

5.3.1 The test case

In order to evaluate our method for heterogeneous media, we studied the evolution of a mode in a spherical cavity made of vacuum which has in its interior a smaller sphere of glass. Material coefficients and radii are indexed by 2 for the big sphere and by 1 for the small one (the two spheres are concentric). Thus, for the electric field,
If $r < a_1$:

$$\left\{ \begin{array}{rcccl} E_x & = & \cos(\omega t) & \dfrac{y}{r^2} & \left(\dfrac{\sin(k_1 r)}{k_1 r} - \cos(k_1 r) \right) \\ E_y & = & \cos(\omega t) & \dfrac{-x}{r^2} & \left(\dfrac{\sin(k_1 r)}{k_1 r} - \cos(k_1 r) \right) \\ E_z & = & 0 & & \end{array} \right.$$

and if $a_1 < r < a_2$:

$$\left\{\begin{array}{rcccc} E_x & = & \alpha\ \cos(\omega t) & \frac{y}{r^2} & \left(\frac{\sin(k_2 r)}{k_2 r} - \cos(k_2 r)\right) \\ E_y & = & \alpha\ \cos(\omega t) & \frac{-x}{r^2} & \left(\frac{\sin(k_2 r)}{k_2 r} - \cos(k_2 r)\right) \\ E_z & = & 0 & & \end{array}\right.$$

For the magnetic induction, if $r < a1$:

$$\left\{\begin{array}{rcccc} Hx & = & \frac{\sin(\omega t)}{\omega \mu_1} & \frac{xz}{r^4} & \left(\sin(k_1 r)\left(\frac{3}{k_1 r} - k_1 r\right) - 3\cos(k_1 r)\right) \\ Hy & = & \frac{\sin(\omega t)}{\omega \mu_1} & \frac{yz}{r^4} & \left(\sin(k_1 r)\left(\frac{3}{k_1 r} - k_1 r\right) - 3\cos(k_1 r)\right) \\ Hz & = & \frac{\sin(\omega t)}{\omega \mu_1} & \left[\frac{z^2}{r^4}\right. & \left(\sin(k_1 r)\left(\frac{3}{k_1 r} - k_1 r\right) - 3\cos(k_1 r)\right) \\ & & & -\frac{1}{r^2} & \left.\left(\sin(k_1 r)\left(\frac{1}{k_1 r} - k_1 r\right) - \cos(k_1 r)\right)\right] \end{array}\right.$$

and if $a_1 < r < a_2$:

$$\left\{\begin{array}{rcccc} Hx & = & \alpha\ \frac{\sin(\omega t)}{\omega \mu_2} & \frac{xz}{r^4} & \left(\sin(k_2 r)\left(\frac{3}{k_2 r} - k_2 r\right) - 3\cos(k_2 r)\right) \\ Hy & = & \alpha\ \frac{\sin(\omega t)}{\omega \mu_2} & \frac{yz}{r^4} & \left(\sin(k_2 r)\left(\frac{3}{k_2 r} - k_2 r\right) - 3\cos(k_2 r)\right) \\ Hz & = & \alpha\ \frac{\sin(\omega t)}{\omega \mu_2} & \left[\frac{z^2}{r^4}\right. & \left(\sin(k_2 r)\left(\frac{3}{k_2 r} - k_2 r\right) - 3\cos(k_2 r)\right) \\ & & & -\frac{1}{r^2} & \left.\left(\sin(k_2 r)\left(\frac{1}{k_2 r} - k_2 r\right) - \cos(k_2 r)\right)\right] \end{array}\right.$$

The continuity of the fields at the interface $r = a_1$ imply that α is a solution of

$$\begin{cases} \alpha = & \dfrac{\dfrac{\sin(k_1 a_1)}{k_1 a_1} - \cos(k_1 a_1)}{\dfrac{\sin(k_2 a_1)}{k_2 a_1} - \cos(k_2 a_1)} \\ \alpha = & \dfrac{\sin(k_1 a_1)\left(\dfrac{3}{k_1 a_1} - k_1 a_1\right) - 3\cos(k_1 a_1)}{\sin(k_2 a_1)\left(\dfrac{3}{k_2 a_1} - k_2 a_1\right) - 3\cos(k_2 a_1)} \\ \alpha = & \dfrac{k_2 \sin(k_1 a_1)}{k_1 \sin(k_2 a_1)} \end{cases}$$

Furthermore one has to choose k_2 so that $k_2 a_2$ is a 0 of same spherical Bessel function j_1 as for the homogeneous sphere in order to fulfill the metallic boundary condition at $r = a_2$. We choose

$$k_2.a_2 = 4.49340$$

We deduce that

$$k_2.a_1 = 3.14159$$

and

$$\alpha = -1$$

So, with $a_1 = 1$ and $a_2 = 1.4303$, we are led to decide that the inside sphere is made of glass with electric permittivity ε_1 equal to $4.\varepsilon_0$ and magnetic permeability μ_1 equal to μ_0 when the outside sphere is made of vacuum with ε_0 and μ_0 as coefficients. Thus :

$$k_1 = 2.k_2$$

5.3.2 Spatial comparison

On figures (13) and (14) one can check that the computations realized with our method give aceptable results. Here, we remark that in the glass part, the mesh has only 5 points by wavelength.

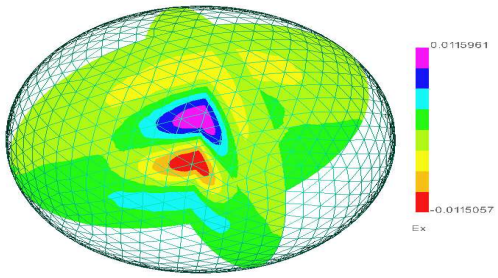

Computed solution

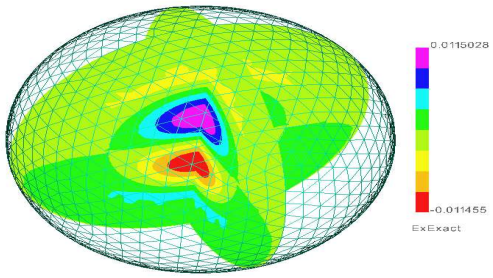

Exact solution

Figure 13: x component of the electric field after 5 periods.

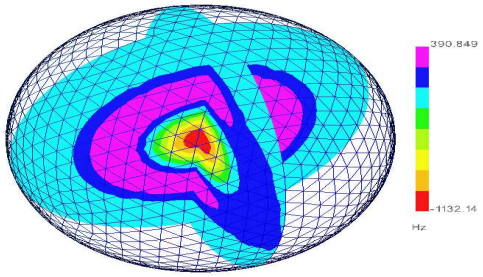

Computed solution

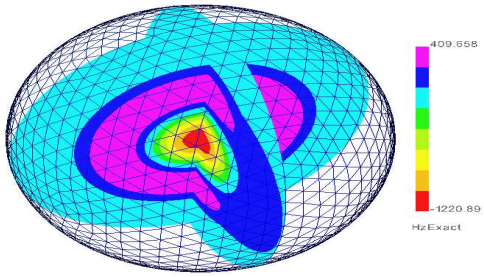

Exact solution

Figure 14: z component of the magnetic field after 5 periods.

5.3.3 Temporal comparison

For this comparison, we check two points, one in the glass and one in the vacuum. We remark that the error is as expected, taken into account that

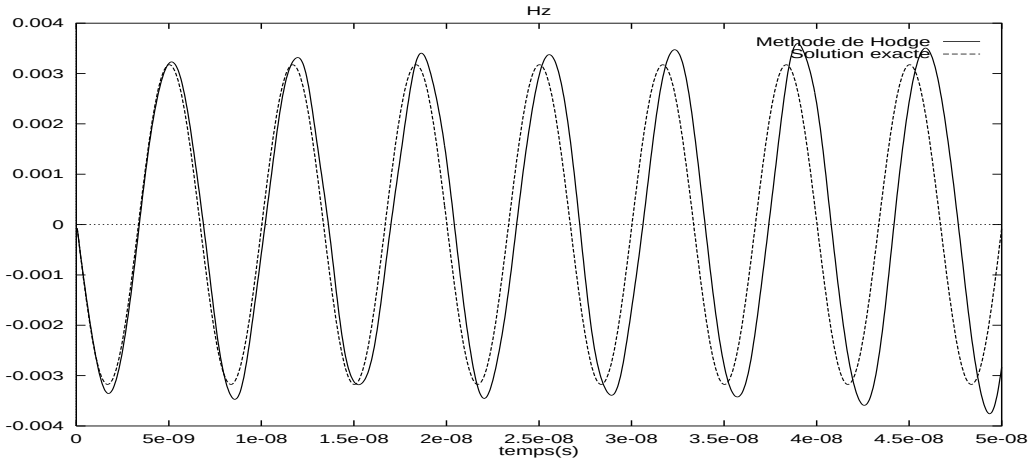

Figure 15: Evolution of the z component of the magnetic field for a point inside glass.

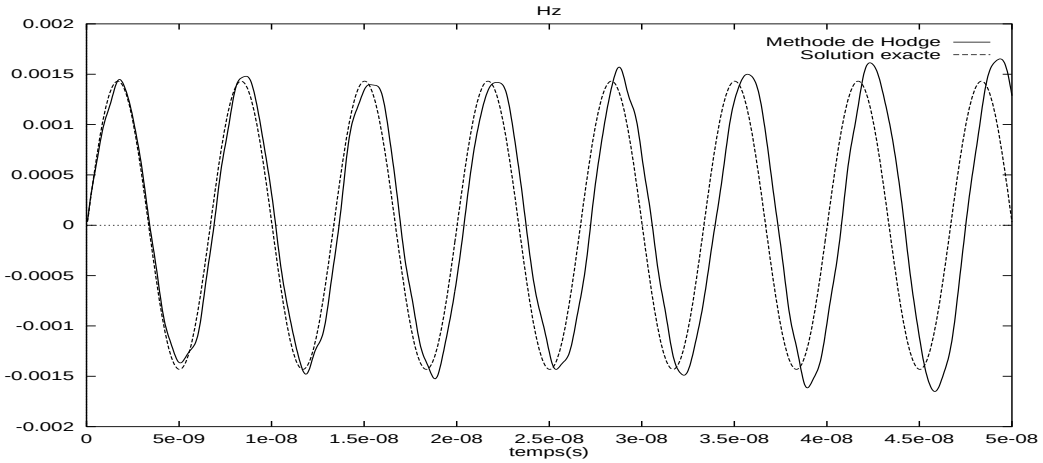

Figure 16: Evolution of the z component of the magnetic field for a point outside of the glass sphere.

the mesh has 5 points by wavelength in the glass and 7 points by wavelength outside. Furthermore, one has to remember that the divergence of the fields are exactly computed.

6 Concluding remarks

The aim of this paper was to present a new discretization of Maxwell system. It is based on a differential geometry approach of these equations and uses Whitney finite elements.

In a first time we have shown the main properties of our scheme :

- It exactly preserves electric and magnetic Gauss laws,
- It exactly preserves a discrete energy,
- the solutions derive from a discrete quadripotential which is an extremum of a discrete Lagrangian,
- It is of order 2 in space and time.

In a second time we have proposed some numerical simulations of resonance modes in various cavities. It appears that the method gives correct results both in short time and long time since the scheme does not loose energy and has a small dispersion. This method is a good one to solve Maxwell system when it is coupled with other equations of physics, like for plasmas, charged particles jets and so on. Nevertheless, it should be a little expensive for simple scattering simulations.

References

[1] D. Anderson, J. Tannehill, and R. Pletcher, *Computational fluid mechanics and heat transfer*, Hemisphere, 1984.

[2] F. Assous, P. Degond, E. Heintze, P. A. Raviart, and J. Segre, *On a finite element method for solving the three dimensional Maxwell equations*, J. Comput. Phys., 109 (1993).

[3] F. Bonnet, *Méthodes de résolution efficace pour le système de Maxwell instationnaire*, thèse de doctorat en mathématiques appliquées, Université de Nice-Sophia-Antipolis, France, 1997.

[4] A. Bossavit, *Un nouveau point de vue sur les éléments mixtes*, MATAPLI, 20 (1989), pp. 23–35.

[5] R. Carpentier, A. de La Bourdonnaye, and B. Larrouturou, *On the derivation of the modified equation for the analysis of linear numerical methods*, M_2AN, 31 (1997), pp. 459–470.

[6] J. P. Cioni, L. Fezoui, and D. Issautier, *High order upwind schemes for solving time-domain Maxwell equations*, La Recherche Aérospatiale, 5 (1994), pp. 319–328.

[7] S. Depeyre, *Stability analysis for finite volume schemes on rectangular and triangular meshes applied to the two-dimensional Maxwell system.* CERMICS, ENPC-INRIA, July 1995.

[8] S. Depeyre and D. Issautier, *A new constrained formulation of the Maxwell system*, M_2AN, (1997).

[9] A. Elmkies and P. Joly, *Éléments finis d'arête et condensation de masse pour les équations de Maxwell : le cas de dimension 3*, C. R. A. S., 325 (1997), pp. 1217–1222.

[10] M. Greenberg, *Lectures on Algebraic topology*, Mathematics lecture note series, W.A.Benjamin, 1967.

[11] R. Harrington, *Time-harmonic electromagnetic fields*, McGraw-Hill book Compagny, 1961.

[12] E. Heintze, *Résolution des équations de Maxwell tridimensionnelles instationnaires par une méthode d'éléments finis conformes*, PhD thesis, Paris, 1992.

[13] S. Lala, *Approximation géométrique des équations de l'élect rodynamique*, mathématiques appliquées, Ecole Nationale des Ponts et Chaussées, June 98.

[14] J. C. Nedelec, *Mixed Finite Elements in $\mathbb{R}^3$*, Numer. Math., 35 (1980), pp. 315–341.

[15] R. W. Noack and D. A. Anderson, *Time Domain Solutions of Maxwell's Equations using a Finite Volume Formulation*, AIAA J., 0451 (1992).

[16] P. A. Raviart and J. M. Thomas, *A mixed finite element method for 2nd order elliptic problems*, Lecture Notes in Mathematics, 606 (1977).

[17] V. Shankar, W. F. Hall, and A. H. Mohammadian, *A Time-Domain Differential Solver for Electromagnetic Scattering Problems*, Proceedings of the IEEE, 77 (1989), pp. 709–721.

[18] Y. I. Shokin, *The Method of Differential Approximation*, Springer Verlag, 1983.

[19] A. Taflove, *Re-Inventing Electromagnetics : Supercomputing Solution of Maxwell's Equations via Direct Time Integration on Space Grids*, AIAA, (1992).

[20] A. Wallace, *Algebraic topology*, International Series of Monographs in Pure and Applied Mathematics, Pergamon Press, 1957.

[21] R. F. Warming and F. Hyett, *The modified equation approach to the stability and accuracy analysis of finite-difference methods*, J. of Comput. Phys., (1974), p. 159.

[22] WorkShop and 2nd International Conference, *Approximations and numerical methods for the solution of the Maxwell's equations*, Washington, 1993.

[23] WorkShop and 3nd International Conference, *Approximations and numerical methods for the solution of the Maxwell's equations*, Oxford, 1995.

[24] K. S. Yee, *Numerical Solution of Initial Boundary Value Problems Involving Maxwell's Equations in Isotropic Media*, IEEE Trans. Antennas and Propagation, 14 (1966), pp. 302–307.

Unité de recherche INRIA Sophia Antipolis
2004, route des Lucioles - B.P. 93 - 06902 Sophia Antipolis Cedex (France)

Unité de recherche INRIA Lorraine : Technopôle de Nancy-Brabois - Campus scientifique
615, rue du Jardin Botanique - B.P. 101 - 54602 Villers lès Nancy Cedex (France)
Unité de recherche INRIA Rennes : IRISA, Campus universitaire de Beaulieu - 35042 Rennes Cedex (France)
Unité de recherche INRIA Rhône-Alpes : 655, avenue de l'Europe - 38330 Montbonnot St Martin (France)
Unité de recherche INRIA Rocquencourt : Domaine de Voluceau - Rocquencourt - B.P. 105 - 78153 Le Chesnay Cedex (France)

Éditeur
INRIA - Domaine de Voluceau - Rocquencourt, B.P. 105 - 78153 Le Chesnay Cedex (France)
http://www.inria.fr
ISSN 0249-6399